[14]R. S. Marjoribanks, M. D. J. Burgess, C. Joshi, G. D. Enright, and M. C. Richardson, Bull. Am. Phys. Soc. 24, 1027 (1979).
[15]A. W. Ehler, F. Begay, T. H. Tan, and P. H. Castine, J. Phys. D 13, L65 (1980).
[16]R. Fedosejevs, M. D. J. Burgess, G. D. Enright, and M. C. Richardson, to be published.
[17]R. F. Benjamin, G. H. McCall, and A. W. Ehler, Phys. Rev. Lett. 42, 890 (1979).
[18]The discussion presented here is similar to that which has been used to explain how vacuum insulation would reduce direct fast-electron preheat of the fuel for laser-fusion targets. See for example, K. Lee, D. W. Forslund, J. M. Kindel, and E. L. Lindman, Nucl. Fusion 19, 1447 (1979).
[19]M. C. Richardson, M. D. J. Burgess, N. H. Burnett, N. A. Ebrahim, G. D. Enright, R. Fedosejevs, P. A. Jaanimagi, C. Joshi, R. S. Marjoribanks, and D. M. Villeneuve, in Proceedings of the Fifth Workshop on Laser Interaction and Related Plasmas, Rochester, edited by Helmut J. Schwarz and Heinrich Hora (to be published).

Study of Ablatively Imploded Spherical Shells

M. H. Key, P. T. Rumsby, and R. G. Evans
Rutherford Laboratory, Chilton, Didcot, Oxfordshire, United Kingdom

and

C. L. S. Lewis, J. M. Ward, and R. L. Cooke
Queen's University, Belfast, United Kingdom
(Received 30 July 1980)

The implosion of spherical-shell targets driven ablatively by six 1.05-μm laser beams at an irradiance of $\sim 10^{13}$ W cm^{-2} has been studied by streak time-resolved x-ray shadowgraphy. Measurements of acceleration determined the ablation pressure. Departures from one-dimensional simulations showed increasingly degraded implosions as the shell aspect ratio $r/\Delta r$ was increased from 10 to 110 for shells with surface perturbations of $\pm 0.05\Delta r$.

PACS numbers: 52.50.Jm, 47.20.+m, 52.55.Mg, 52.70.-m

Compression of plasma in laser-driven implosions has been characterized as "ablative" or "exploding pusher" according to the relative importance of surface ablation pressure and bulk pressure due to preheating by electrons. To date, experimental study of ablative implosions has been limited,[1] partly because their high-density low-temperature plasma yields little diagnostic information in the form of x-ray or fusion-product emission compared with exploding-pusher implosions.[2] The development of x-ray probing techniques[3] has alleviated this problem and permitted study of the implosion dynamics of spherical-shell targets under ablative acceleration with use of streak time-resolved x-ray shadowgraphy.[4]

Elementary mechanics show that for negligible mass loss, a spherical shell with ratio of radius to wall thickness (aspect ratio) $r/\Delta r$ and density ρ can be accelerated to a velocity v of the order $(P_a r/\Delta r)^{1/2}$ by a surface ablation pressure P_a. Since the stagnation pressure P_f of the implosion is of the order ρv^2 it follows that $P_f \propto P_a r/\Delta r$. High aspect ratio therefore leads to high stagnation pressure. However, the acceleration of the dense shell by the low-density ablation plasma is subject to the Rayleigh-Taylor instability, whose classical growth exponent for perturbations of wavelength $\lambda \sim \Delta r$ is approximately $(2\pi r/\Delta r)^{1/2}$ during an implosion. Since the instability growth depends on the aspect ratio it is expected to limit the maximum aspect ratio and stagnation pressure. Detailed theoretical work has, however, yielded contradictory results, some finding growth rates close to classical[5] and some predicting stabilizing effects due to factors not considered in the classical Rayleigh-Taylor theory such as thermal conduction and ablation flow through the unstable region.[6] Such contradictions emphasize the value of experimental study of the stability of ablative implosions of shells of increasing aspect ratio as described here.

Our experimental arrangement is illustrated in Fig. 1. Six beams of 1.05-μm laser light irradiate the microballoon target and a seventh is focussed on a horizontal Al-foil x-ray-backlighting target. The microballoon is viewed along a hori-

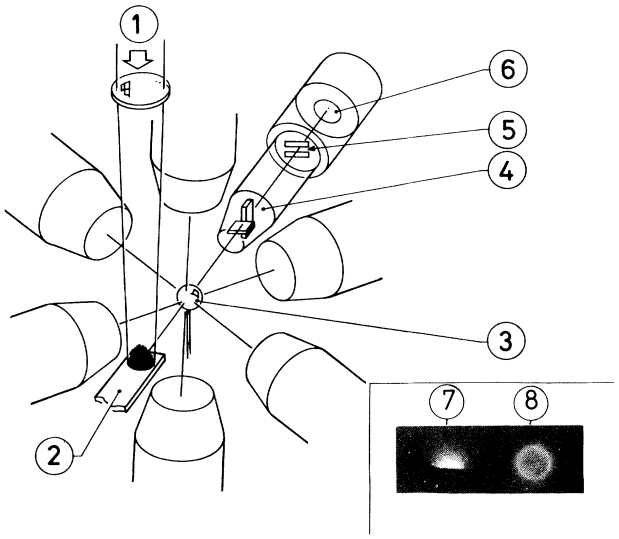

FIG. 1. Apparatus. 1 and 2, x-ray backlighting laser beam and target; 3, microballoon; 4, x-ray microscope; 6, x-ray streak camera and 5, its slit; 7, x-ray pinhole camera image of backlighting plasma; and 8, of microballoon plasma.

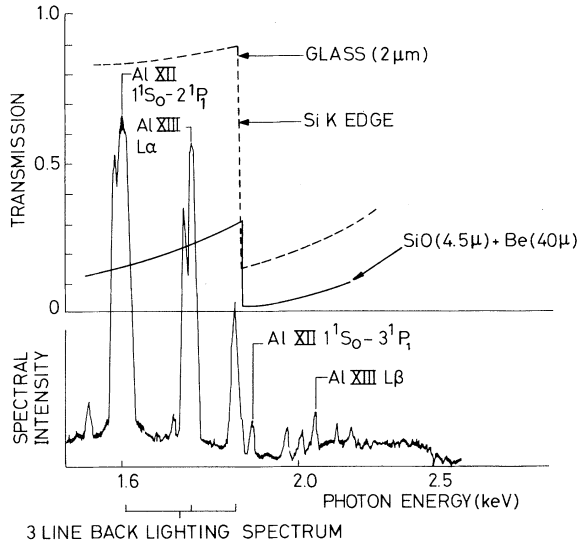

FIG. 2. Spectrum of the backlighting plasma (lower graph) recorded via an SiO filter with spectral transmission shown in the upper graph (solid line) together with transmission of a typical microballoon (dashed line).

zontal axis against the x-ray emission from the backlighting target by a Kirkpatrick-Baez x-ray microscope which projects a 15 times magnified image onto the CsI photocathode of an x-ray streak camera. A 30-μm wide field in the target is selected by a horizontal slit and streaking of the image gives 80-ps temporal resolution. Additional diagnostics include an absolutely calibrated, space-resolving, x-ray spectrometer to characterize the backlighting spectrum, and a pinhole camera to determine the relative brightness of backlighting and shell emission and to observe the uniformity of irradiation of the shell (see inset 8 in Fig. 1).

The laser delivered 40 J to the backlighting beam and 6×15 J to the microballoon target in pulses of 0.8-ns rise time and 1.5-ns full width at half maximum. Ablative implosions were obtained by irradiating the microballoons at 5×10^{12} to 10^{14} W cm^{-2}. The backlighting target was irradiated in a 500-μm focal spot at 10^{13} W cm^{-2}. Observations were made via an SiO filter whose Si-K edge, together with the 2.2 keV cutoff of the x-ray microscope mirrors, reduced the effective backlighting spectrum to the three circa 1.6 keV x-ray resonance lines from Al XII and Al XIII ions shown in Fig. 2. The Si-K edge of the filter also selectively suppressed the Si XIII and Si XIV resonance line emission of glass microballoons. Since the backlighting photon energies were in the K transmission window of Si, their penetration through glass was good and their simple spectrum made calculation of target opacity[3] straight forward.

The apparatus was used to record streaked shadowgraphs of unirradiated microballoons. Densitometry of the results showed that the instrumental spatial resolution was 17 μm and that measured and computed profiles of x-ray opacity in the microballoon[6] were in agreement.

Figure 3 shows examples of the results obtained with ablatively imploded empty microballoons for 3 cases: (a), (b), and (c) of aspect ratio 12, 43, and 110, respectively. These implosions had the following parameters: $r=93$, 134, and 142 μm, respectively; $\Delta r=6.6\,\mu$m (CH) + 1.1 μm (glass), 2 μm (CH) + 1 μm (glass), and 1.3 μm (glass), respectively; irradiance $I=2.5\times10^{13}$, 10^{13}, and 5×10^{12} W cm^{-2}, respectively. These combinations of parameters gave a similar implosion time close to the end of the laser pulse in each case. The surface roughness of the targets was approximately $\pm0.05\Delta r$ for wavelengths similar to the shell thickness. Irradiation nonuniformity was $\pm40\%$ on a scale of a few microns due to structure in the laser beams and $\pm20\%$ on the larger scale associated with the six-beam irradiation. The backlighting pulse was delayed by 0.9 ns to display the trajectory of the boundary of the absorbing region and its minimum diameter.

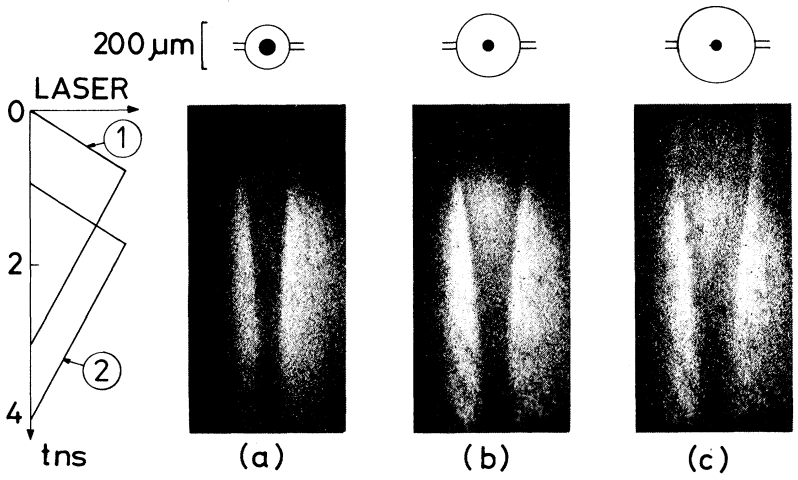

FIG. 3. (a), (b), and (c) are streaked x-ray shadowgraphs of implosions with parameters given in the text. Sketches above streaks show to scale the initial target diameter and (in black) the calculated minimum diameter of the core of opacity $\tau \geq 1$. 1 and 2 are the laser pulses irradiating the microballoon and backlighting targets, respectively.

The thickest shell with 6.6 μm plastic coating (a) shows no discernable self-emission prior to the backlighting or transmission of backlighting x rays through its center. The boundary of the opaque region is as sharp as the instrumental resolution. A thinner shell (b) shows significant transmission of backlighting x rays early in the implosion as expected theoretically but, because of its plastic coating, no self-emission. The thinnest uncoated glass shell (c) shows weak self-emission prior to the backlighting, strong transmission of the backlighting x rays in the early part of the implosion as expected theoretically, but an increasingly diffuse and irregular boundary to the absorbing region. In Fig. 3(c) the sharpness of the shell boundary, defined as the distance for a 10% to 90% change in transmission, increases from the 17 μm instrumental limit at $t = 0$ to 55 μm at $t = 600$ ps. These numbers are from densitometry of the negatives which was also used to determine the trajectory of the boundary of the opaque region where the opacity $\tau \geq 1$. This is plotted in Fig. 4 for case (c). The implosions were also simulated with a one-dimensional Lagrangian fluid code MEDUSA[3] to obtain $\tau \geq 1$ trajectories as shown in Fig. 4. Experiments and simulations were in good agreement in the acceleration phase of the implosion, enabling a determination of the ablation pressure P_a at the peak of the laser pulse both from the computer

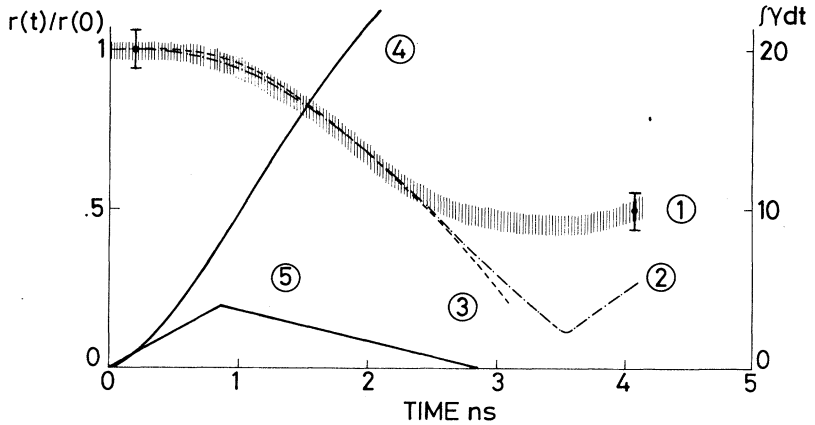

FIG. 4. Analysis of case (c). 1 and 2, trajectories $r(t)/r(0)$ of the boundary of opacity $\tau \geq 1$; 1 is measured, 2 is calculated. 3, an analytic model fit to the trajectory; 4, classical Rayleigh-Taylor growth exponent for wavelength $\lambda = \Delta r$; 5, laser pulse.

simulations and from fitting an analytically calculated trajectory by assuming $P_a(t) = K[I(t)]^{2/3}$ to determine K. The latter is also shown in Fig. 4. The ablation pressure thus measured was 1.3 Mbars in case (c). This and additional data were in fair agreement with other less direct measurements of P_a.[4]

Measured implosion times were consistent with numerical simulations (see, e.g., Fig. 4), but comparisons of the measured and calculated radius of the opaque core revealed major discrepancies. The latter are illustrated in Fig. 3 by the scale diagrams from simulations set above the streak records. The ratio of measured to computed minimum diameter of the region of opacity $\tau \geq 1$ is 1.6, 3.4, and 4.2 for cases (a), (b), and (c), respectively. Figure 4 shows case (c) in more detail. It has the largest aspect ratio ($r/\Delta r = 110$) and the largest discrepancy, with the measured diameter of the opaque core implying a volume 80 times larger than predicted by the simulation. This together with the observed diffuse and irregular boundary to the opaque region suggest some kind of breakup of the shell during the implosion. A compilation of data given in Fig. 5 shows a systematic increase with aspect ratio of the discrepancy between measured and computed opaque core radius.

Preheating effects are unlikely to explain this discrepancy since numerical simulation with a fraction of the laser energy dumped uniformly in the shell showed that even with the improbably large value of 10% preheating in case (c) above, the computed opaque core radius was still 2 times smaller than the measured value.

Nonuniformity of irradiation causes local variation in the ablation pressure and thus in the implosion velocity. Very crudely it may be estimated that an opaque core radius of $r_0/2$ could be produced if parts of the shell traveled to the center and "bounced" to $r_0/2$ while slower parts traveled only to $r_0/2$. One-dimensional numerical calculations suggest this requires an irradiance variation of 5:1. The experimental irradiance nonuniformity discussed above is considerably less than this.

Rayleigh-Taylor instability may amplify small-scale surface irregularities on the shells and also velocity perturbations driven by hot spots or filamentation in the laser beam, although thermal conduction will help to reduce the effects of nonuniform irradiation on small scale lengths. Maximum instability is expected for irregularities in a spatial scale $\lambda \sim \Delta r$ and our targets had surface irregularities of $\pm 0.05\Delta r$ on this scale. Figure 4 shows how the classical growth exponent reaches 20 at the point where the measured implosion trajectory departs strongly from the simulation. Thus even growth rates much less than classical could produce a large effect from an initial amplitude of $0.1\Delta r$. Small-scale instabilities would probably make the boundary of the opaque core appear diffuse and irregular as in the high-aspect-ratio implosion shown in Fig. 3(c). It appears, therefore, that the observed failure of high-aspect-ratio shells to implode satisfactorily may be predominantly due to Rayleigh-Taylor amplification of both small-scale irregularities of the shell surface and of perturbations originating from illumination nonuniformity.

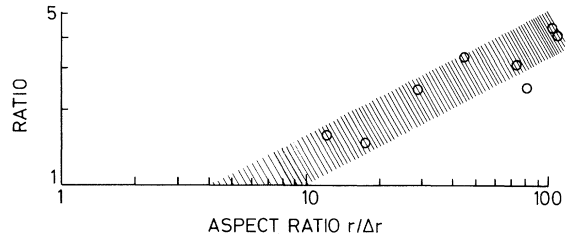

FIG. 5. Ratios of measured to calculated minimum diameters of the core of opacity $\tau \geq 1$ as a function of target aspect ratio $r/\Delta r$.

[1]N. G. Basov *et al.*, Pis'ma Zh. Eksp. Teor. Fiz. 23, 474–477 (1976) [JETP Lett. 23, 428 (1976)]; D. Billon *et al.*, in *Laser Interaction and Related Plasma Phenomena*, edited by H. J. Schwartz and H. Hora (Plenum, New York, 1977), Vol. 4A, p. 503.

[2]E. K. Storm *et al.*, Phys. Rev. Lett. 40, 1570 (1978); D. T. Attwood, IEEE J. Quantum Electron. 14, 909 (1978).

[3]M. H. Key, C. L. S. Lewis, J. G. Lunney, A. Moore, T. A. Hall, and R. G. Evans, Phys. Rev. Lett. 41, 1467 (1978).

[4]M. H. Key *et al.*, Science Research Council Rutherford Lab Reports No. RL-79014, 1979 (unpublished), and No. RL-80023, 1980 (unpublished).

[5]J. D. Lindl, W. C. Mead, Phys. Rev. Lett. 34, 1273 (1975); R. E. Kidder, Nucl. Fusion 16, 3 (1976); S. E. Bodner *et al.*, in *Proceedings of the Seventh International Conference on Plasma Physics and Controlled Nuclear Fusion Research, Innsbruck, Austria, 1978* (International Atomic Energy Agency, Vienna, Austria, 1979), Vol. III, p. 17.

[6]Yu V. Afanasev *et al.*, Pis'ma Zh. Eksp. Teor. Fiz. 21, 150–155 (1975) [JETP Lett. 21, 68 (1975)]; R. L. McCory and R. L. Morse, Phys. Fluids 19, 175 (1975); K. A. Brueckner, S. Jorna, and R. Janda, Phys. Fluids 22, 1841 (1979).

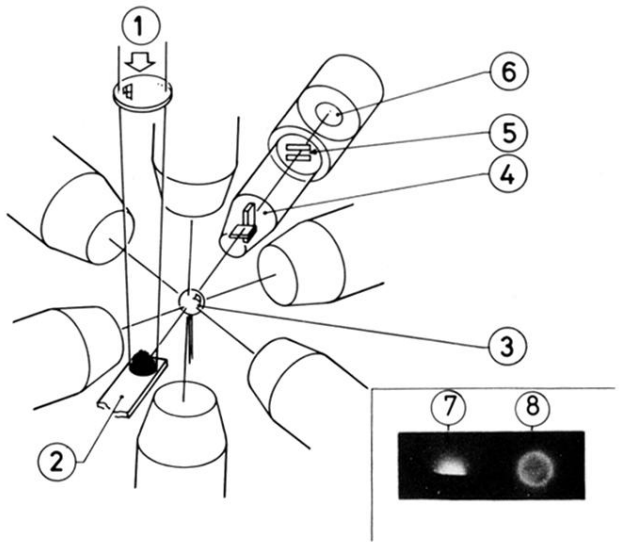

FIG. 1. Apparatus. 1 and 2, x-ray backlighting laser beam and target; 3, microballoon; 4, x-ray microscope; 6, x-ray streak camera and 5, its slit; 7, x-ray pinhole camera image of backlighting plasma; and 8, of microballoon plasma.

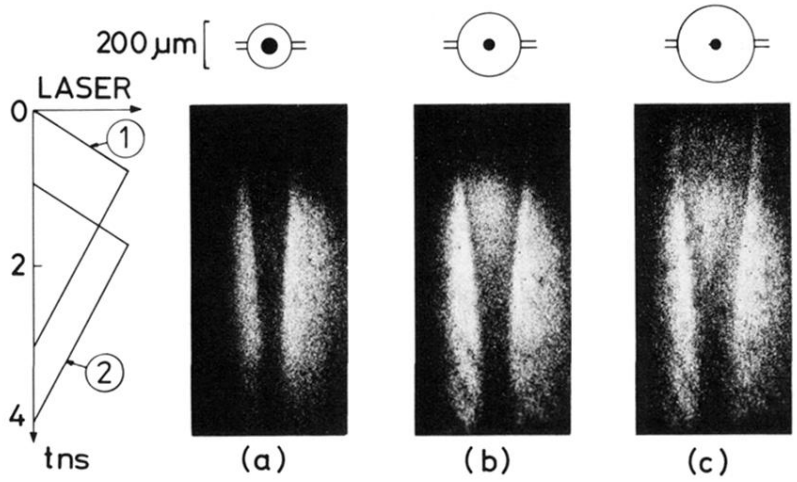

FIG. 3. (a), (b), and (c) are streaked x-ray shadowgraphs of implosions with parameters given in the text. Sketches above streaks show to scale the initial target diameter and (in black) the calculated minimum diameter of the core of opacity $\tau \geq 1$. 1 and 2 are the laser pulses irradiating the microballoon and backlighting targets, respectively.